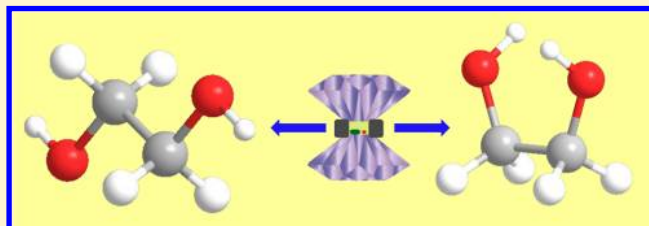


# Hydrogen Bonds and Conformations in Ethylene Glycol under Pressure

Chitra Murli,<sup>†</sup> Ning Lu, Zhaohui Dong, and Yang Song\*

Department of Chemistry, University of Western Ontario, London, Ontario, N6A5B7, Canada

**ABSTRACT:** Ethylene glycol (EG) is a model system for studying complex hydrogen bonding networks in biological compounds such as polysaccharides and sugars. Using in situ high-pressure Raman and infrared absorption spectroscopy, we have investigated the pressure induced variation in the conformations and hydrogen bonding interactions in this compound up to 10 GPa. The high-pressure behavior of Raman modes suggests that EG exists as a liquid with a mixture of trans and gauche conformations up to 3.1 GPa. At  $\sim 4$  GPa, a liquid–solid transition is evidenced by the appearance of external Raman modes as well as visual observation. Raman and infrared spectra of EG at high pressures indicate that new hydrogen bonding networks are formed prior to liquid–solid transition and the high pressure phase is stabilized to gauche conformation at pressures above 5 GPa.



## INTRODUCTION

Ethylene glycol (EG) is an interesting compound from the point of view of structural chemistry, as it has several conformations<sup>1,2</sup> with different hydrogen bonding networks. It serves as a model system for studying complex intramolecular and intermolecular hydrogen bonding interactions in biologically significant compounds such as polysaccharides and sugars.<sup>3,4</sup> It has several industrial applications due to its highly viscous nature, which is attributed to its uniform and less mobile three-dimensional hydrogen bonding network in comparison to water.<sup>5,6</sup>

Under compression, when molecules are brought closer, they reorient themselves to counter steric hindrances and facilitate close packing, which subsequently results in new crystal structures. Pressure is therefore known to induce conformational changes, structural transformations, polymerization, variation in the hydrogen bonding interactions such as making and breaking of hydrogen bonds, proton disorder, symmetrization, and so on.<sup>7–13</sup> Hence, one can explore new high-pressure phases of EG that may have conformations and hydrogen bonds that are not accessible at ambient conditions or at lower temperatures. Although many diffraction, spectroscopic measurements, and computational theories are available at ambient pressures,<sup>14–23</sup> no detailed high-pressure investigations<sup>24</sup> are reported for EG. We have carried out high-pressure Raman and infrared absorption spectroscopic investigations of EG up to 10 GPa and report significant changes in the conformations and hydrogen bonding interactions in EG under pressure.

Conformations and hydrogen bonding interactions of EG (chemical formula  $C_2H_6O_2$ ) in the vapor, liquid, and solid forms have been studied by many investigators using theoretical, diffraction, and spectroscopic methods.<sup>4,14–20</sup> An EG molecule is a triple rotor about the O–C, C–C, and C–O bonds. As each can assume three significant conformational positions, this molecule can exist as 27 conformers, and out of

these 10 are unique.<sup>6</sup> Among these, some of the gauche conformers are found to favor intramolecular hydrogen bonding interactions, whereas in the trans conformation these interactions are not favored, as can be seen from Figure 1.<sup>1,2</sup> At

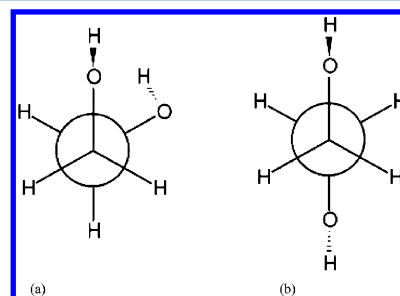


**Figure 1.** Conformations of EG: (a) gauche; (b) trans.

ambient conditions, most of the spectroscopic studies reveal that the liquid phase of EG has a mixture of trans and gauche conformations, and its solid phase is stabilized by gauche conformation.<sup>18,19</sup> Some of the spectroscopic investigations of EG at different temperatures reported evidences of intramolecular hydrogen bonds in the gauche conformation.<sup>19,20</sup>

However, the existence of intramolecular hydrogen bonding interactions in EG has been a subject of debate over several decades.<sup>1,2,14–20</sup> Bako et al. have identified the conformers of the EG molecule as gauche OCCO arrangement stabilized by intramolecular hydrogen bond using X-ray, neutron diffraction, and density functional theory.<sup>15</sup> However, a recent study by Chopra et al. based on X-ray diffraction and electron density

**Received:** June 25, 2012

**Revised:** September 1, 2012

**Published:** September 17, 2012

measurements obtained at 100 K reports that the crystal structure is stabilized by a network of intermolecular O–H···O hydrogen bonds, and there is no topological evidence for intramolecular hydrogen bonding interactions even in the gauche conformation.<sup>16</sup> Under compression, as one can obtain new phases that are not accessible at ambient conditions, we have investigated high-pressure behavior of EG using Raman and infrared spectroscopy. In this manuscript, we report spectroscopic signatures, which suggest that EG is stabilized to gauche conformation at higher pressures with new hydrogen bonding networks of possible intramolecular origin.

## EXPERIMENTAL DETAILS

A symmetric diamond anvil cell equipped with a pair of type I diamonds with a culet size of 400  $\mu\text{m}$  was used in the experiment. The liquid samples of EG obtained from Sigma-Aldrich were loaded into a hole with a diameter of 150  $\mu\text{m}$  drilled on a stainless steel gasket that was preindented to a thickness of 90  $\mu\text{m}$ . The pressure was determined using the well-established ruby fluorescence line with an uncertainty of  $\pm 0.05$  GPa under quasi-hydrostatic conditions.<sup>25</sup> Raman measurements were carried out with a customized Raman microspectroscopy system. The 488 nm line of an Innova Ar<sup>+</sup> laser from Coherent Inc. was used as the excitation source. The laser was focused to less than 5  $\mu\text{m}$  on the sample with an average power of 30 mW by an Olympus microscope with a 20 $\times$  objective. A 15 $\times$  eyepiece and a digital camera allowed for the precise alignment of the focused laser beam on the sample. The Raman scattering signal was collected by the same objective lens with a backscattering geometry. The Rayleigh scattering was removed by a pair of notch filters which enabled a measurable spectral range above 150  $\text{cm}^{-1}$ . The scattered photons were focused on the entrance slit of a spectrometer and then dispersed by an imaging spectrograph (from Acton Research Corporation) housing a monochromator with a 0.5 m focal length and equipped with multiple gratings. In this experiment, a 1800 lines/mm grating with 0.1  $\text{cm}^{-1}$  resolution was used. The Raman signal was recorded by an ultrasensitive liquid nitrogen-cooled back-illuminated charge coupled device (CCD) detector from Acton. The system was calibrated using neon lines with an uncertainty of  $\pm 1$   $\text{cm}^{-1}$ . All measurements were conducted at room temperature. For infrared absorption measurements, a customized IR microspectroscopy system that constitutes a Fourier transform infrared (FTIR) spectrometer from Bruker Optics Inc. (model Vertex 80v) equipped with a Global IR light source was used. A collimated IR beam of varying diameter set with apertures ranging from 0.25 to 8 mm was directed into a relay box through a KBr window on the spectrometer. The beam was then focused on to the sample in the diamond anvil cell by an iris optics and 15 $\times$  reflecting objective lens with a numerical aperture of 0.4. The transmitted IR beam was collected using another identical reflecting objective as the condenser and was directed to a midband mercury cadmium telluride (MCT) detector equipped with a ZnSe window that allows measurements in the spectral range 600–12000  $\text{cm}^{-1}$ .

## RESULTS AND DISCUSSION

The Raman and infrared spectra of liquid EG have been recorded in the entire spectral region of interest, and the observed modes are found to be consistent with earlier spectroscopic investigations reported in the litera-

ture.<sup>17–21,26–33</sup> We have taken assignments of most of the observed Raman and infrared modes from the work of Krishnan et al. and Matsuura et al.<sup>18,19</sup> The assignments of all the Raman and infrared modes are shown in their respective plots at ambient conditions. Although several Raman studies have been reported in the literature, the assignment of C–C stretching mode is quite contradictory.<sup>18,19,27,29</sup> Table 1 gives the list of the observed Raman modes for liquid phase at ambient pressures and solid phase at 7 GPa, their assignments, and their variation with pressure.

**Table 1. Assignments and Pressure Dependence of Raman Modes of Liquid and Solid EG**

liquid phase at 0.1 MPa <sup>a</sup>		assignments		solid phase III at 7 GPa <sup>a</sup>	
$\nu$ ( $\text{cm}^{-1}$ )	$d\nu/dp$ ( $\text{cm}^{-1}/\text{GPa}$ )	liquid <sup>b</sup>	solid III <sup>a</sup>	$\nu$ ( $\text{cm}^{-1}$ )	$d\nu/dp$ ( $\text{cm}^{-1}/\text{GPa}$ )
			external mode	175	5.0
			external mode	202	5.4
			external mode	243	7.4
			C–C–O torsion	333	8.4
350	12.0	C–C–O bend		382	3.5
482	4.3	C–C–O bend (trans)	C–C–O bend (gauche)	579	1.6
524	6.4	C–C–O bend (gauche)	C–C–O bend (gauche)	592	3.7
			O–H torsion	709	8.6
865	5.9	C–C stretch		888	3.7
			C–C stretch	903	5.8
			C–C stretch	927	5.1
1036	5.2	C–O stretch	C–O stretch	1058	1.1
1064	8.1	C–O stretch (trans)	C–O stretch (trans)	1100	1.4
1091	3.7	CH <sub>2</sub> rock	CH <sub>2</sub> rock	1117	1.8
1210	8.0	CH <sub>2</sub> twist	CH <sub>2</sub> twist	1241	2.0
1265	2.5	CH <sub>2</sub> twist	CH <sub>2</sub> twist	1273	1.5
1381		COH bend	COH bend	1408	0.8
1397		COH bend	COH bend	1487	0.8
1460	3.8	CH <sub>2</sub> sciss	CH <sub>2</sub> sciss	1526	0.4
2719		combination	combination	2741	0.1
2877	15.9	CH <sub>2</sub> sym stretch	CH <sub>2</sub> stretch	2990	5.8
			CH <sub>2</sub> stretch	3035	8.0
			CH <sub>2</sub> stretch	3057	7.8
2939	10.6	CH <sub>2</sub> asym stretch	CH <sub>2</sub> stretch	3084	9.6
3347		OH stretch	OH stretch	3156	
			OH stretch	3227	
			OH stretch	3275	–12.5

<sup>a</sup>This study. <sup>b</sup>References 18 and 19.

When liquid EG is compressed to pressures above  $\sim 4$  GPa, it is found to crystallize as shown in the photographs presented in Figure 2. The Raman spectra of EG at different pressures during compression in the spectral region 200–3600  $\text{cm}^{-1}$ , excluding the diamond peaks, are shown in Figure 3. The Raman spectra at different pressures during decompression are given in Figure 4. The variation of Raman shifts with pressure is presented in Figure 5. Infrared spectra of EG at different pressures during compression are shown in Figure 6. Variations in the frequencies of infrared active OH stretching modes with pressure are presented in Figure 7. While the spectral changes

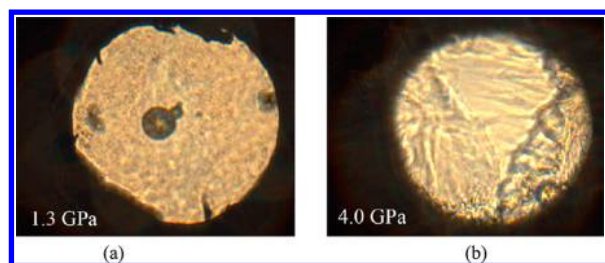


**Figure 2.** Photographs of liquid EG in a diamond anvil cell under pressure at 1.3 GPa (a) and during crystallization at  $\sim 4$  GPa (b) collected via an optical microscope.

in the Raman modes provide information on conformational changes, the high pressure behavior of infrared active OH stretching modes are quite informative with regard to pressure induced changes in the hydrogen bonding interactions.

**A. Raman Spectra of EG up to 5 GPa.** As shown in Figure 3 persistence of the broad Raman modes up to 3.1 GPa indicates that this compound exists in the liquid phase up to this pressure. No discernible Raman modes were observed  $<400$   $\text{cm}^{-1}$  up to this pressure. However, around 4 GPa, consistent with the visual observation shown in Figure 2, the formation of solid crystal structure is indicated by the replacement of broad Raman modes of the liquid phase by sharper ones. In addition, new modes appear in the spectral region 150–400  $\text{cm}^{-1}$ . These modes are very weak compared to the other Raman modes. The changes in the external modes are non-monotonic in the pressure range 3–5 GPa. As seen from Figures 3 and 5, the C–C–O bending mode observed at 357  $\text{cm}^{-1}$  initially stiffens (blue shifts) at a rate of 12  $\text{cm}^{-1}/\text{GPa}$  and softens (red shifts) across 4 GPa upon crystallization. Among the C–C–O bending modes at 484  $\text{cm}^{-1}$  and 529  $\text{cm}^{-1}$ , the mode at 484  $\text{cm}^{-1}$  is found to be stronger in the trans conformation (trans band), and the mode at 529  $\text{cm}^{-1}$  is found to be stronger in the gauche form (gauche band). The trans band stiffens at rate of 4.3  $\text{cm}^{-1}/\text{GPa}$  up to 3 GPa. These modes reveal significant changes in the conformations in the pressure range 3–5 GPa. As one can see from Figure 3a, initially the trans band is found to be dominant at 4 GPa, and trans and gauche coexist at 5 GPa.

C–C stretching mode, which is observed as a broad band centered around 868  $\text{cm}^{-1}$ ,<sup>18,19</sup> stiffens at rate of 5.9  $\text{cm}^{-1}/\text{GPa}$ . CO stretching modes at 1042, 1070, and 1091  $\text{cm}^{-1}$  stiffen at a rate 5.2, 8.1, and 3.7  $\text{cm}^{-1}/\text{GPa}$  respectively.<sup>18,19</sup> In the high pressure spectra, as seen from Figure 3, above 3.1 GPa, there is increase in the relative intensity of the modes observed at 1042  $\text{cm}^{-1}$  and 1070  $\text{cm}^{-1}$ , and in addition, a new sharp mode is observed close to 1100  $\text{cm}^{-1}$ . CH<sub>2</sub> scissoring mode is observed as a single band at 1463  $\text{cm}^{-1}$  and stiffens at a rate of 3.8  $\text{cm}^{-1}/\text{GPa}$ . Above 3.1 GPa it is replaced by three peaks that continue to exist up to 4 GPa. However at pressures above 5.1 GPa, two new bands appear and continue to remain up to the highest pressure 10.6 GPa of our study. Other modes that are observed are CH<sub>2</sub> twist at 1210  $\text{cm}^{-1}$ , 1265  $\text{cm}^{-1}$ , and CH<sub>2</sub> wag at 1290  $\text{cm}^{-1}$ , which stiffen under pressure. The bands observed at 2882 and 2937  $\text{cm}^{-1}$  are symmetric and antisymmetric CH<sub>2</sub> stretching vibrations, respectively. As seen from Figure 3b, significant changes have also been noted in these spectra. Above 3.1 GPa, we observe that these two broad bands are replaced by four bands. Two new modes at 3138  $\text{cm}^{-1}$  and 3238  $\text{cm}^{-1}$ , which are relatively sharper, appear in the O–H stretching region in the Raman spectra at pressures above 3

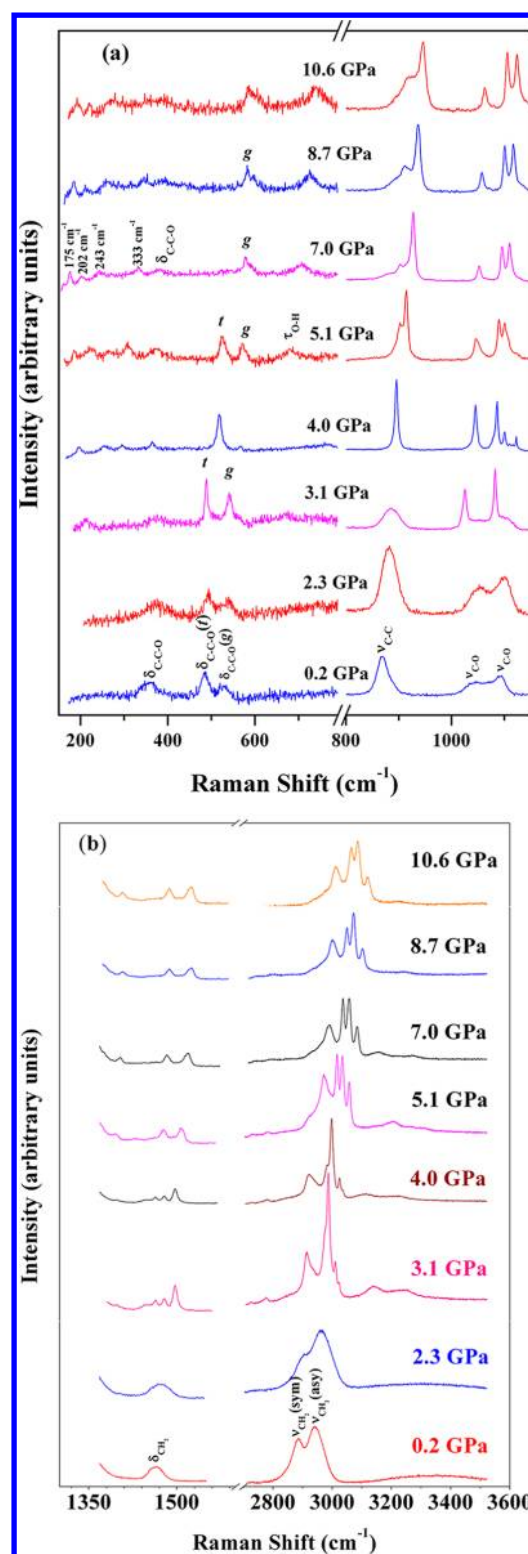


**Figure 3.** Raman spectra of EG at different pressures under compression: (a) in the spectral region of 200–1200  $\text{cm}^{-1}$ ; (b) in the spectral region of 1400–3600  $\text{cm}^{-1}$ . Assignments of Raman modes of the liquid phase at 0.2 GPa and solid phase at 7 GPa are shown:  $\nu$  - stretch;  $\delta$  - bend;  $g$  denotes gauche;  $t$  represents trans.

GPa. In the pressure range 3–5 GPa, there are nonmonotonic changes in the number and positions of these bands. At 3 GPa they are found at 3139 and 3248  $\text{cm}^{-1}$ . At 4 GPa, they are observed at 3112  $\text{cm}^{-1}$  and 3230  $\text{cm}^{-1}$ , respectively.



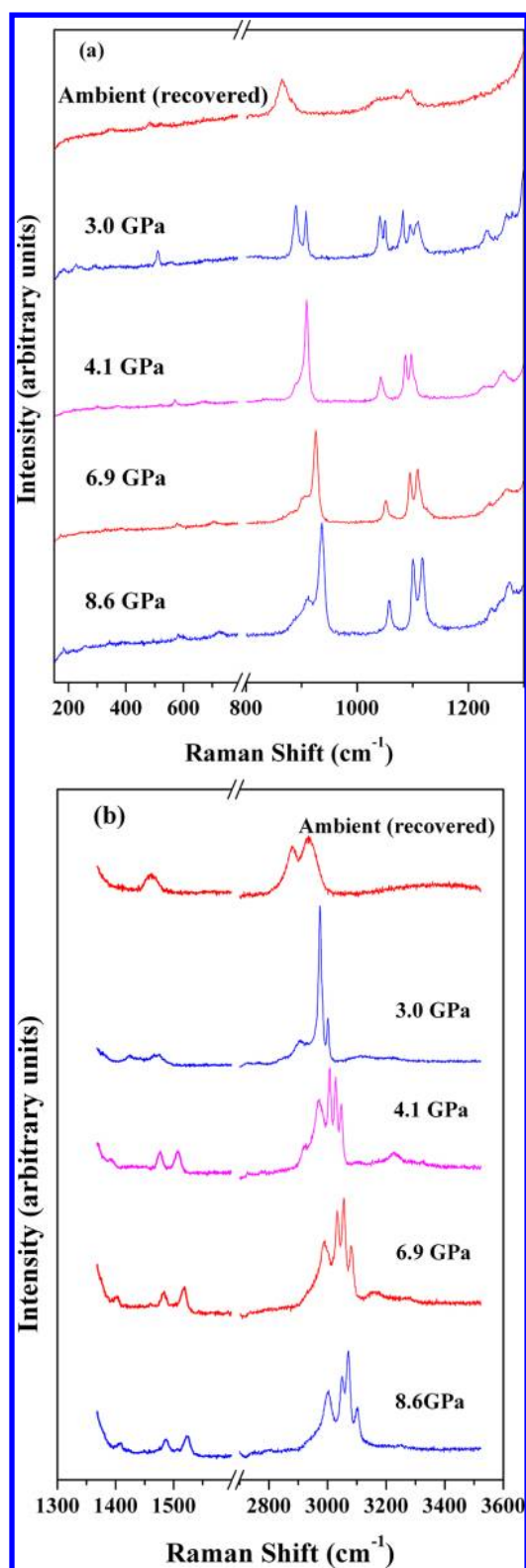


**Figure 4.** Raman spectra of EG at different pressures under decompression: (a) in the spectral region of 200–1200  $\text{cm}^{-1}$ ; (b) in the spectral region of 1400–3600  $\text{cm}^{-1}$ .

**B. Raman Spectra of EG at 5–7 GPa.** At pressures above 5 GPa, a new Raman mode emerges at 680  $\text{cm}^{-1}$ . This mode is reported to be associated with the O–H torsional mode and is observed in the infrared spectrum, whereas it is absent in the Raman spectrum of EG at ambient conditions.<sup>19,21</sup> This is

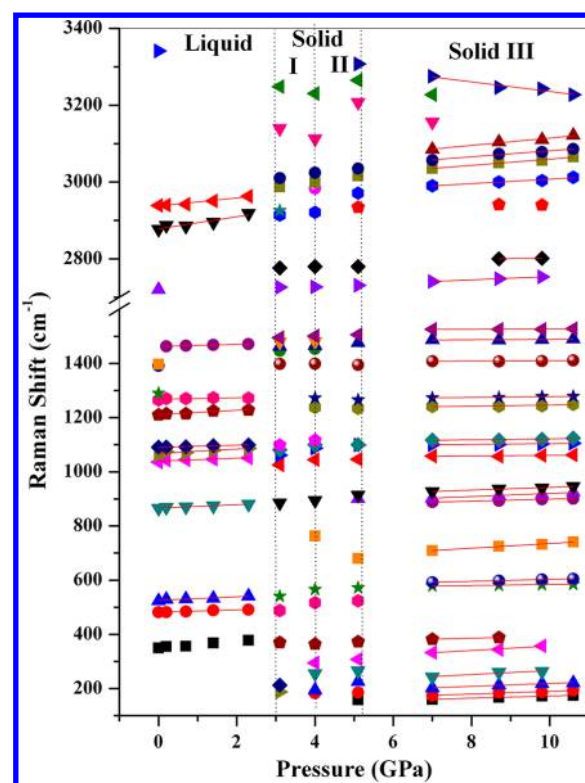


**Figure 5.** Pressure dependence of Raman shifts of EG. Lines are drawn as a guide to the eye.

because in the trans form, this mode is forbidden in the Raman spectra due to inversion symmetry and the mutual exclusion principle. However, in the gauche conformation, there is no center of inversion, and the mutual exclusion rule is no longer applicable. Hence, emergence of this infrared active mode in the Raman spectra at 5 GPa indicates that EG is stabilizing to gauche conformation.<sup>21</sup> Above 7 GPa, this mode shows a relatively larger pressure-induced stiffening of 7.9  $\text{cm}^{-1}/\text{GPa}$ , and the relative intensity of this mode increases with pressure. Also, above 5 GPa, a systematic pressure induced stiffening of the external modes up to 10 GPa suggests that the structure is stabilized to gauche conformation, which is also indicated by the persistence of the gauche band (529  $\text{cm}^{-1}$ ) and the absence of the trans band (484  $\text{cm}^{-1}$ ).

The profiles of  $\text{CH}_2$  vibrational modes at 5 and 7 GPa fairly resemble the calculated profiles for gauche conformations of EG.<sup>32</sup> The number of modes and the total separation of the lowest and highest of these four bands is nearly 94  $\text{cm}^{-1}$ , which is very close to that reported for a dimer.<sup>33</sup> Above 5 GPa, three relatively sharper bands are observed in the O–H stretching region at 3304  $\text{cm}^{-1}$ , 3265  $\text{cm}^{-1}$ , and 3205  $\text{cm}^{-1}$ , which soften at a rate of 17  $\text{cm}^{-1}/\text{GPa}$ , 24  $\text{cm}^{-1}/\text{GPa}$ , and 24  $\text{cm}^{-1}/\text{GPa}$  up to 7 GPa, respectively. All the observed spectral changes are found to be completely reversible, as shown in Figure 4.

**C. FTIR Spectra of EG under Pressure.** We have recorded infrared absorption spectra of EG in the entire spectral region 600–4000  $\text{cm}^{-1}$ . Figure 6 gives the infrared spectra at different pressures under compression, and the pressure induced variation in the peak positions of the OH stretching bands is presented in Figure 7. As shown in Figure 6b, the OH stretching infrared active mode is observed as a very broad band at 3347  $\text{cm}^{-1}$  at ambient conditions, and there is no discernible asymmetry or any fine structure. As this band is very broad, it

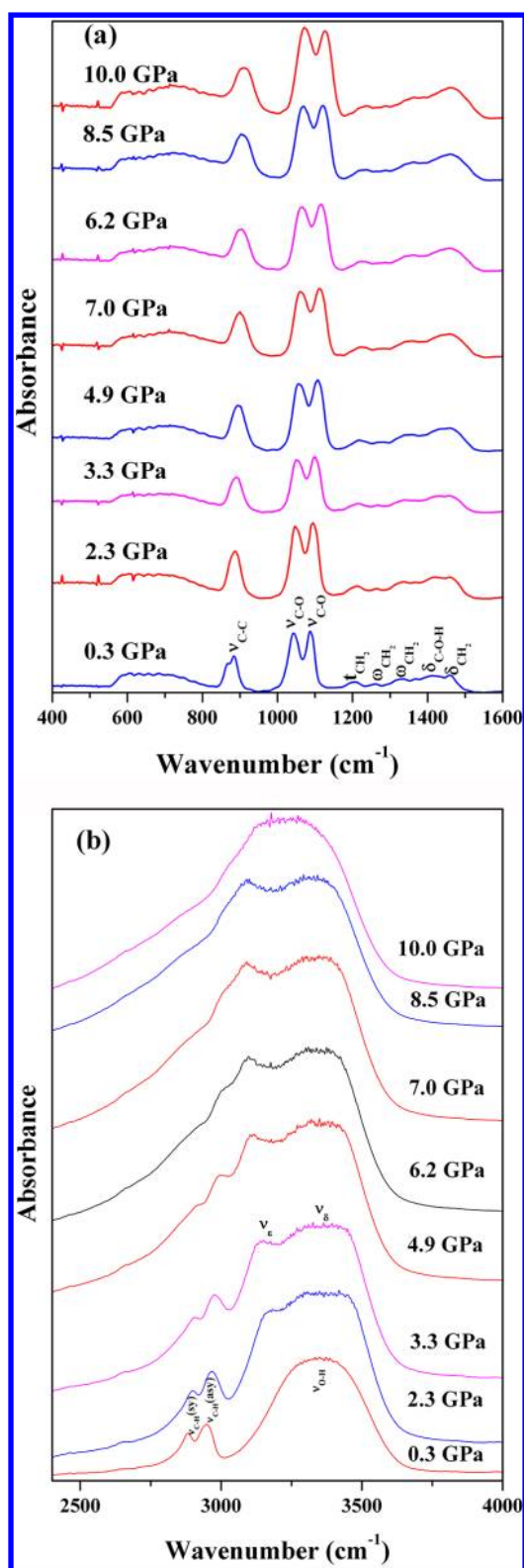


**Figure 6.** IR absorption spectra of EG at different pressures under compression: (a) in the spectral region of 400–1600  $\text{cm}^{-1}$ :  $\nu$  - stretch;  $\omega$  - wag;  $\tau$  - torsion;  $\delta$  - bend;  $t$  - twist; (b) in the spectral region of 2500–4000  $\text{cm}^{-1}$ .

was not possible to fit, and we have taken the central band position as the peak position to get an approximate of its evolution with pressure. As one can see from Figure 7, this mode shows a red shift at the rate of  $\sim 4.5 \text{ cm}^{-1}/\text{GPa}$  up to 2

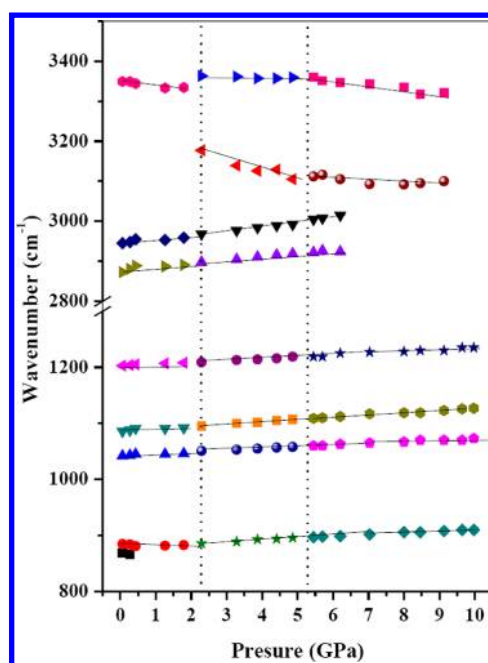


**Figure 7.** Pressure dependence of IR active modes of EG. Lines are drawn as a guide to the eye.

GPa, a discontinuous blue shift by  $27 \text{ cm}^{-1}$  across 3 GPa, red shift at the rate of  $\sim 9 \text{ cm}^{-1}/\text{GPa}$  in the pressure range 4–7 GPa, and a large red shift at a rate  $\sim 36 \text{ cm}^{-1}/\text{GPa}$  at pressures above 7 GPa. At higher pressures above 2.3 GPa, a new band appears at  $\sim 3174 \text{ cm}^{-1}$ , which is analogous to  $\nu_e$  reported by Crupi et al.<sup>20</sup> This mode is found to soften at a rate of  $31 \text{ cm}^{-1}/\text{GPa}$  and is observed at  $3143 \text{ cm}^{-1}$  at 3.3 GPa. It may be noted here that this is very close to the new OH mode ( $3139 \text{ cm}^{-1}$ ) observed in the Raman spectra at 3.1 GPa. This mode continues to soften up to 7 GPa. The red shift of this mode in the pressure range 4–7 GPa is about  $84 \text{ cm}^{-1}$  ( $28 \text{ cm}^{-1}/\text{GPa}$ ). The high pressure behavior of this mode is very different from that of the main infrared active mode originally observed at  $3347 \text{ cm}^{-1}$ , which shows a red shift of  $24 \text{ cm}^{-1}$  ( $8 \text{ cm}^{-1}/\text{GPa}$ ) in the same pressure range. The diverse high pressure behavior of these two bands indicates that they are arising from different kinds of hydrogen bonds. There are also some weak fine structures observed around  $3293 \text{ cm}^{-1}$ .

**D. Structural and Conformational Changes of EG under Pressure.** The high-pressure behavior of Raman modes of EG indicates that EG is in the liquid phase up to 3.1 GPa.<sup>18,19</sup> In addition, the observation of trans and gauche C–C–O bending modes suggests that EG continues to exist in liquid form with a mixture of trans and gauche conformations up to this pressure. Above 4 GPa, liquid–solid transition is noted by the visual observation and emergence of sharper Raman modes in place of broad Raman modes of the liquid phase. In addition, many new modes appear in the spectral region  $150\text{--}400 \text{ cm}^{-1}$ . In the pressure range 4–5 GPa, non-monotonic changes observed in many of the Raman modes suggest that the solid phase in this pressure range has different conformations and hydrogen bonding networks and is not yet stabilized. Above 5 GPa, the appearance of the O–H torsional mode, which is otherwise forbidden in the Raman spectra, the absence of the trans band, and the persistence of the gauche band suggest that the high pressure phase III is stabilized to gauche conformation above this pressure.

**E. Hydrogen Bonds in EG under Pressure.** Appearance of relatively sharper Raman modes in the O–H stretch region of the Raman spectra suggests that new hydrogen bonds are formed. Such sharp features are generally observed for nonlinear hydrogen bonds, which, in some cases, can be intramolecular hydrogen bonds. Observation of these new modes just prior to liquid–solid transition and subsequent stabilization of gauche conformation suggests that the new hydrogen bonding networks may have intramolecular origin. This is also supported by the appearance of new modes in the region 150–400  $\text{cm}^{-1}$ . While the intermolecular hydrogen bond stretching modes are observed at  $< 200 \text{ cm}^{-1}$ , intramolecular hydrogen bond modes can be expected to extend up to 400  $\text{cm}^{-1}$ .<sup>34</sup>

At this point, it is also of interest to compare the nature of changes in conformations and hydrogen bonds of EG in different chemical environments. Krueger et al. have investigated the spectroscopic behavior of EG in dilute solution of  $\text{CCl}_4$  as a function of temperature and have discussed the possibility of intramolecular cyclic hydrogen bonds.<sup>17</sup> However, in this compound, OH stretching frequency corresponding to the linear intermolecular hydrogen bond and that of the bent intramolecular bond are reported to be nearly the same. EG is found to prefer a folded gauche form with an internal hydrogen bond in the presence of Xe solvent.<sup>35</sup> Crupi et al. resolved the broad infrared OH band of EG observed at 55 °C into three bands.<sup>20</sup> The lowest frequency band  $\nu_e$  is associated with OH vibrations involved in the intramolecular hydrogen bond of the monomeric structures, whereas  $\nu_\delta$  arises from OH stretching vibration where both oxygen and hydrogen atoms are involved in an intermolecular hydrogen bond with the neighboring units, giving rise to trimers and more extended structures, and  $\nu_\gamma$  is associated with OH vibrations in which oxygen (hydrogen) bonds with the hydrogen (oxygen) of another molecule forming dimeric structures.

Comparing our results with that of Crupi et al.,<sup>20</sup> the lower infrared band  $\nu_e$  at 3145  $\text{cm}^{-1}$ , which emerged at pressures above 2 GPa, may be associated with the new hydrogen bond, which may have intramolecular origin, and the main broad OH infrared band  $\nu_\delta$  at 3347  $\text{cm}^{-1}$  arises from intermolecular hydrogen bonds. The red shift of the new infrared active mode  $\nu_\delta$  and the increase in its width and relative intensity up to 5 GPa suggest that the gauche conformation is stabilized through these hydrogen bonds. However, at pressures above 5 GPa, once the gauche conformation is stabilized,  $\nu_e$  does not show softening anymore, while  $\nu_\delta$  is found to show larger softening  $\sim 36 \text{ cm}^{-1}/\text{GPa}$ , which suggests that the strength of the intermolecular hydrogen bond may increase above 7 GPa. Although the red shift of O–H stretching modes indicate strengthening of hydrogen bonds in some cases,<sup>36</sup> the correlation of the O–H frequency with the strength of the corresponding O–H...O hydrogen bond is not trivial and is found to be system specific.<sup>37</sup> The knowledge of the hydrogen bond parameters at higher pressures are therefore required to confirm our spectroscopic results. High-pressure structural and theoretical investigations of EG will therefore be very useful to get a complete picture of the hydrogen bonding networks at higher pressures.

## CONCLUSIONS

Our high-pressure Raman spectroscopic studies reveal that EG exists in liquid phase, which has both trans and gauche conformations up to 3.1 GPa. At pressures above 4 GPa,

liquid–solid transition is noted by visual observation under a microscope and the replacement of broad Raman modes of the liquid phase by sharper modes of solid phase. In the pressure range 4–5 GPa, non-monotonic changes in the observed Raman modes suggest that high pressure phases are not stabilized up to this pressure. Above 5 GPa, the appearance of O–H torsional mode which is otherwise forbidden in the Raman spectra, the absence of the trans band, and the persistence of the gauche band suggest that the solid structure is stabilized to gauche conformation above this pressure. Observation of new sharper Raman and infrared modes in the OH stretching region prior to the liquid–solid transition suggests that new hydrogen bonding networks are formed, which may have intramolecular origin. The red shift of the new infrared active mode and increase in its width and the relative intensity up to 5 GPa suggests that stabilization of gauche conformation may be brought by the new hydrogen bonding networks. The observed changes in the conformations and hydrogen bonding interactions are found to be completely reversible upon release to ambient conditions.

## AUTHOR INFORMATION

### Corresponding Author

\*E-mail: yang.song@uwo.ca; phone: 519-661-2111 ext 86310; Fax 519-661-3022.

### Present Address

<sup>†</sup>High pressure and Synchrotron Physics Division, Bhabha Atomic Research Centre, Mumbai 400085 (e-mail: cmurli@barc.gov.in).

### Notes

The authors declare no competing financial interest.

## ACKNOWLEDGMENTS

This work was supported by a Discovery Grant, a Research Tools and Instruments Grant from the Natural Science and Engineering Research Council of Canada, the Leaders Opportunity Fund from the Canadian Foundation for Innovation, and an Early Researcher Award from the Ontario Ministry of Research and Innovation. C.M. is very thankful to Dr. T. Sakuntala, for her valuable suggestions. C.M. acknowledges the Centre for Chemical Physics (CCP) Fellowship from the University of Western Ontario.

## REFERENCES

- (1) Crittenden, D. L.; Thompson, K. C.; Jordan, J. T. M. *J. Phys. Chem. A* **2005**, *109* (12), 2971–2977.
- (2) Howard, D. L.; Jorgensen, P.; Kjaergaard, H. G. *J. Am. Chem. Soc.* **2005**, *127*, 17096–17103.
- (3) Bosco, M.; Picotti, F.; Radoicovich, R. *Biopolymers* **2000**, *53*, 272–280.
- (4) Guvench, O.; Mackerell, A. D., Jr. *J. Phys. Chem. A* **2006**, *110*, 9934–9939.
- (5) Cramer, C. J.; Truhlar, D. G. *J. Am. Chem. Soc.* **1994**, *116*, 3892–3900.
- (6) Rodnikova, M. N.; Chumaevskii, N. A.; Troitskii, V. M.; Kayumova, D. B. *Russ. J. Phys. Chem.* **2006**, *80*, 826–830.
- (7) Dong, Z.; Beilby, N. G.; Huang, Y.; Song, Y. *J. Chem. Phys.* **2008**, *128*, 074501–9.
- (8) Sabharwal, R. J.; Huang, Y.; Song, Y. *J. Phys. Chem. B* **2007**, *111*, 7267–7273.
- (9) Mishra, A. K.; Murli, C.; Garg, N.; Chitra, R.; Sharma, S. M. *J. Phys. Chem. B* **2010**, *114*, 17084–17090.
- (10) Murli, C.; Song, Y. *J. Phys. Chem. B* **2010**, *114*, 9744–9749.



- (11) Aoki, K.; Yamawaki, H.; Sakashita, M.; Fujihisa, H. *Phys. Rev. B* **1996**, *54*, 15673–15677.
- (12) Goncharov, A. F.; Struzhkin, V. V.; Somayazulu, M.; Hemley, R. J.; Mao, H. K. *Science* **1996**, *273*, 218–220.
- (13) Hemley, R. J. *Annu. Rev. Phys. Chem.* **2000**, *51*, 763–800.
- (14) Podo, F.; Nemethy, G.; Indovina, P. L.; Radics, L.; Viti, V. *Mol. Phys.* **1974**, *27*, 521–539.
- (15) Bako, I.; Grosz, T.; Palinkas, G.; Bellissent-Funel, M. C. *J. Chem. Phys.* **2003**, *118*, 3215–3221.
- (16) Chopra, D.; Guru Row, T. N.; Arunan, E.; Klein, R. A. *J. Mol. Struct.* **2010**, *964*, 126–133.
- (17) Krueger, P. J.; Mettee, H. D. *J. Mol. Spectrosc.* **1965**, *18*, 131–140.
- (18) Krishnan, K.; Krishnan, R. S. *Proc. Indian Acad. Sci.* **1966**, *64*, 111–122.
- (19) Matsuura, H.; Hiraishi, M.; Miyazawa, T. *Spectrochim. Acta* **1972**, *28 A*, 2299–2304.
- (20) Crupi, V.; Majolino, D.; Migliardo, P.; Venuti, V. *Mol. Phys.* **2000**, *98*, 1589–1594.
- (21) Matsuura, H.; Miyazawa, T. *Bull. Chem. Soc. Jpn.* **1967**, *40*, 85–94.
- (22) Thalladi, V. R.; Boese, R.; Weiss, H. C. *Angew. Chem., Int. Ed.* **2000**, *39*, 918–922.
- (23) Buckley, P.; Giguere, P. A. *Can. J. Chem.* **1967**, *45*, 397–407.
- (24) Budzianowski, A.; Katrusiak, A. In *High-Pressure Crystallography*; Katrusiak, A., McMillan, P. F., Eds.; Springer, 2004; pp 157–168.
- (25) Mao, H. K.; Xu, J.; Bell, P. M. *J. Geophys. Res.* **1986**, *9*, 4673–4676.
- (26) Maleknia, S.; Friedman, B. R.; Abedi, N.; Schwartz, M. *Spectrosc. Lett.* **1980**, *13*, 777–784.
- (27) Sawodny, W.; Niedenzu, K.; Dawson, J. W. *Spectrochim. Acta* **1967**, *23A*, 799–806.
- (28) Luo, R.; Jonas, J. J. *Raman Spectrosc.* **2001**, *32*, 975–978.
- (29) Akhihisa, M. *J. Am. Chem. Soc.* **1960**, *82*, 3040–3043.
- (30) Pruettingkura, P.; Ho, S.; Schwartz, M. *Spectrosc. Lett.* **1979**, *12*, 679–685.
- (31) Chumaevskii, N. A.; Rodnikova, M. N.; Barthel, J. *J. Mol. Liq.* **2004**, *115*, 63–67.
- (32) Hommel, E. L.; Merle, J. K.; Ma, G.; Hada, C. M.; Allen, C. H. *J. Phys. Chem. A* **2005**, *109*, 811–818.
- (33) Zubkova, O. B.; Shabadash, A. N. *J. Appl. Spectrosc.* **1971**, *14*, 639–643.
- (34) Nibbering, E. T. J.; Dreyer, J.; Luhn, O.; Bredenbeck, J.; Hamm, P.; Elsaesser, T. Vibrational dynamics of hydrogen bonds. In *Analysis and Control of Ultrafast Photoinduced Reactions*; O. Kühn, L. Wöste (Eds.); Springer Series in Chemical Physics; Springer Verlag: Heidelberg, Germany, 2007; Vol. 87, p 622.
- (35) Hayashi, H.; Tanaka, H.; Nakanishi, K. *Fluid Phase Equilib.* **1995**, *104*, 421–430.
- (36) Nakamoto, K.; Margoshes, M.; Rundle, R. E. *J. Am. Chem. Soc.* **1955**, *77*, 6480–6486.
- (37) Sikka, S. K.; Sharma, S. M. *Phase Transitions* **2008**, *81*, 907–934.